Steady-State Motion Visual Evoked Potentials with 3D Stimuli in a VR-Based BCI

Hanneke A. Scheppink[1,2], María del Carmen Cortés Navarro[1] and Ivan Volosyak[1,2]

***Abstract*— This study investigated the potential of steady-state motion visual evoked potential (SSMVEP) using 3D stimuli as a preliminary step towards developing a brain-computer interface (BCI) for command selection in a virtual reality (VR) environment. Several movement patterns and stimulus shapes were examined to determine the optimal stimulus configurations for eliciting strong and robust SSMVEP responses. The aim was to identify the most effective stimulus and SSMVEP movement to improve user comfort, interaction and control accuracy for future immersive VR applications presented in a head-mounted display (HMD). The proposed shapes, cube and diamond, yielded comparable performance in the steady-state visual evoked potential (SSVEP) condition; however, for the zooming and rotating movements, the cube achieved higher average accuracies. In the frequency spectrum, the average signal-to-noise ratio (SNR) values of the diamonds were comparable to those of the cubes. Subjective results showed that participants had a preference for the rotating diamonds.**

I. Introduction

A brain-computer interface (BCI) is a technology that enables real-time communication between the human brain and external devices by translating brain signals into commands. The neural activity is commonly measured non-invasively with electroencephalography (EEG) [1]. The visual evoked potential (VEP) is a brain response triggered by a specific external visual stimulus, commonly used in BCIs to encode certain action commands. Specifically, one of the fundamental VEP-based BCIs is the steady-state VEP (SSVEP) BCI. Here, stimuli flicker with specific constant frequencies, evoking a brain response matching the attended stimulus' frequency and its harmonics [1]. Using EEG to record these signals, they can be decoded to classify the attended stimulus and perform a certain action. However, traditional SSVEP stimuli can cause visual fatigue and discomfort due to the high-contrast flickering [2]. To address this, the steady-state motion VEP (SSMVEP) paradigm was introduced, in which the stimuli move with a smooth and constant graphical motion at a specific frequency, eliciting a similar response as SSVEP [2]. The continuous movement of the stimuli is perceived as more comfortable than the flickering, and induces less fatigue [2], [3].

Traditionally, SSMVEP stimuli are presented on a computer screen, limiting their applications. Recently, the integration of SSVEP and SSMVEP stimuli with virtual reality (VR) and augmented reality (AR) has gained increasing attention. VR environments can create more immersive experiences, leading to increased user engagement compared to traditional display methods [4]. Furthermore, SSVEP BCIs in VR have demonstrated better system performance than standard desktop versions [5].

Although the integration of SSVEP-based BCIs with VR has been explored in various applications, such as ankle rehabilitation [6], a VR maze game [4], and remote robot control [5], research on this topic remains relatively limited. Moreover, most studies on SSMVEP in virtual environments have focused on AR applications rather than fully immersive VR settings, often using planar stimulation targets in two-dimensional (2D) scenes or three-dimensional (3D) environments [7], [8], [9]. The use of SSMVEP in VR has so far been investigated with 2D objects, where the stimuli were placed on a black bar at the top of the VR environment [10]. To the best of our knowledge, no study has specifically examined the use of SSMVEP on 3D objects and its implementation in a VR setting. This gap highlights the need for further investigation into the benefits and challenges of integrating SSMVEP-based BCIs into immersive VR environments. This integration has great potential in rehabilitation, entertainment, and assistive technologies, allowing for more comfortable and prolonged use by reducing visual fatigue, improving immersion through smoother interactions, and improving control accuracy for more intuitive and accessible BCI applications.

The current study aims to develop SSMVEP-based 3D motion stimuli for integration into a fully immersive VR environment to enable BCI-driven control. This was done by studying two different 3D shapes with two different SSMVEP motions. Specifically, the aim was to compare the 3D version of the often used 2D squares, so cubes, and a 3D shape that is easily distinguishable in a 3D virtual environment. Here, a diamond shape was chosen. As motions, zooming and rotating were selected. Additionally, for both shapes the SSVEP protocol was implemented, specifically, flickering the stimuli at the same frequencies used for SSMVEP. This approach allows us to compare and optimise the stimulus design for future applications in interactive and immersive SSMVEP-based VR-BCI systems.

II. Methods and Materials

A. Participants

In the study, 12 healthy subjects (8F, 4M, average age of 25.6±3.5, between 20-31) participated in the experiment. All had normal or corrected-to-normal vision. Seven participants reported having previous experience with a BCI system.

[1]Faculty of Technology and Bionics, Rhine-Waal University of Applied Sciences, 47533 Kleve, Germany

[2]Department of Informatics and Data Science, Graduate School for Applied Research in North Rhine-Westphalia (PK NRW), 44801 Bochum, Germany ivan.volosyak@hochschule-rhein-waal.de

Before the experiment, the participants received elaborate information about the experimental procedure and any possible involved risks. Participants had the opportunity to opt-out at any time during the experiment. Those who agreed to participate in this study signed a consent form and were financially compensated after participation. The study was designed and conducted in accordance with the Helsinki Declaration. The study was approved by the ethical committee of the medical faculty of Duisburg-Essen University (24-11957-BO). All data were stored anonymously.

B. Hardware

The used computer (Dell Precision Desktop with an NVIDIA RTX3070 graphics card) operated on Microsoft Windows 10 Education running on an Intel processor (Intel i9, 3.70 GHz). The head-mounted display (HMD) used in this study was the HTC Vive Pro (HTC Corporation, Taoyuan, Taiwan), with a combined resolution of 2880×1600 pixels (1440×1600 pixels per eye), a 90 Hz vertical refresh rate, and a 110° visual angle.

EEG data was acquired with the g.tec g.USBamp amplifier (g.tec, Shiedlberg, Austria) using sixteen gel-based passive scalp electrodes, placed according to the international 10-5 system at the following positions: P_7, P_3, P_z, P_4, P_8, PO_7, PO_3, PO_z, PO_4, PO_8, O_1, O_z, O_2, O_9, I_z, and O_{10}. The ground and reference electrodes were placed at C_z and AF_z, respectively. The EEG signals were recorded with the amplifier using a sampling frequency Fs of 600 Hz. With abrasive electrode gel, impedances were kept below 5 kΩ.

C. Stimulus Presentation

The experimental stimulus environment presented in the HMD was designed using the Unity game engine (Unity Technologies, San Francisco, CA, USA), version 6000.0.31f1 [11]. Two distinct 3D shapes were created, specifically, a cube and a diamond. The cubes served as 3D counterparts to the commonly used 2D square stimuli, while the diamonds were introduced as a novel design, chosen for their ease of recognition within immersive virtual reality environments. To create a more complex stimulus to induce stronger responses, a checkerboard texture was applied to both shapes. The diamonds were as wide and deep as the cubes at their widest point, and slightly higher than the cubes. At any time during the experiment, four targets were presented in the environment, in a 2-by-2 design, see Figure 1. In the VR environment, the virtual camera was positioned at the central point of the 2-by-2 stimulus grid. Head tracking was disabled, thereby fixing the participant's general viewpoint to this central location, and ensuring it remained centred on the stimuli throughout the experiment.

Next to different 3D stimulus shapes, two different motions were tested. Specifically, zooming in and out, so increasing and decreasing the size of the stimulus, and rotating where the stimulus was rotated back and forth. To determine if these motions could serve as a feasible alternative to the effective, yet often uncomfortable, SSVEP paradigm, SSVEP flickering was also implemented for both shapes.

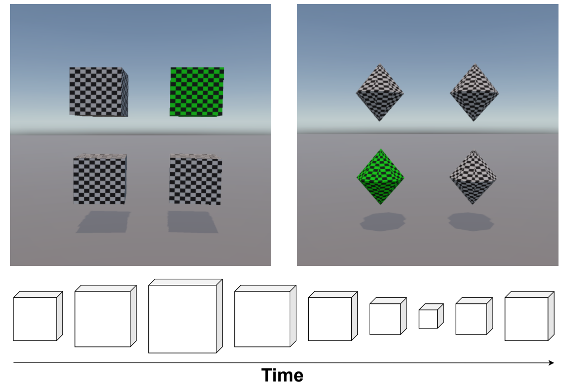

Fig. 1: **The VR stimulation environment and stimuli presented to the participants in the HMD.** The top line of the figure presents the VR environment shown to the participant with either the cube (left) or diamond shape (right), the cueing is also shown in green. The lower line shows a graphical example of the movement modulation.

To implement the motions, specific frequencies had to be chosen with respect to the HMD vertical refresh rate ($V_{RR} = 90$ Hz). Specifically, such that the frequencies had an equal number of frames in both directions of the motion behaviour. To ensure a smooth movement, the frequency could not be too high since that reduces the number of steps in one movement direction. This led to the following base-frequencies for the stimulation: $3.214, 4.500, 5.625$, and 7.500Hz. Where the highest frequency of $f_t = 7.5$ Hz, meant the full period was $V_{RR}/f_t = 90/7.5 = 12$ frames, so 6 frames for each movement direction. This is somewhat low, however, the choices for the frequencies with this HMD's refresh rate were quite limited. The movements followed the trigonometric function $sin((2\pi * f_t * i)/V_{RR}$, where f_t is the base-frequency, i is the frame index, and V_{RR} the refresh rate of the HMD. A graphical representation of the zooming movement with this function is presented at the bottom of Figure 1. The four frequencies were encoded to the 2-by-2 stimuli, from left to right, top to bottom.

As described above, the SSVEP paradigm was also implemented, in which a stimulus flickers according to a constant frequency. Here, SSVEP was applied such that the stimulus was flickering between the checkerboard texture and solid black. The base-frequencies used for SSVEP stimulation were the same as described above for SSMVEP.

D. Offline Recording

To collect the EEG data, participants were instructed to focus for 3 s on a target that was prior cued in green for 2 s, see Figure 1. All four targets were cued and observed in sequence. This was done for six blocks, in which for each a target was observed once, resulting in $6 \times 4 = 24$ trials per condition. After one trial ended, the next target was immediately cued, after which the flickering or moving started. Participants answered a questionnaire after each condition, before proceeding to the next condition. Before processing the EEG data, a notch filter was applied at $50\,\text{Hz}$ and a bandpass filter between $1\,\text{Hz}$ and $100\,\text{Hz}$.

E. Frequency Responses

The common average reference (CAR) is a spatial filtering method that can be used to increase the signal-to-noise ratio (SNR) by reducing noise [12]. This is done by subtracting the average value of all electrodes from the electrode of interest, here Oz, as it usually shows the strongest response [13]:

$$V_i^{CAR} = V_i - \frac{1}{m}\sum_{j=1}^{m} V_j, \tag{1}$$

where V_i is the selected electrode signal, m the number of channels (the $m = 15$ remaining channels), and V_i^{CAR} the re-referenced signal.

The frequency spectrum was computed using Fast Fourier Transform (FFT). The spectral power was estimated using Welch's method with a Hann window. The SNR was then computed as the ratio of power in a certain frequency bin. Here, the SNR was extracted for the frequency spectrum between 1 and $40\,\text{Hz}$.

F. Signal Processing

Here, a filter bank canonical correlation analysis (FBCCA) was used to analyse the data offline, for more details on FBCCA for SSVEP analysis, please see [14]. For SSVEP- or SSMVEP-based BCIs, CCA is often used to find a linear transformation that maximises the correlation between the cosine and sine templates of the stimulus frequency (f_t) and its N_h harmonics, and the recorded EEG signal. To create the reference signals $\mathbf{Y}_{f_t}$ for each stimulation frequency f_t, $N_h = 2$ harmonics were used in this study, see [14]. The recorded EEG signals for one trial $\mathbf{X}$ were compared to each of the $\mathbf{Y}_{f_t}$ reference signals using CCA. This resulted in:

$$\max_{\mathbf{w}_X,\mathbf{w}_Y} \rho(\mathbf{x},\mathbf{y}) = \frac{\mathbf{w}_X^T \mathbf{X}\mathbf{Y}^T \mathbf{w}_Y}{\sqrt{\mathbf{w}_X^T \mathbf{X}\mathbf{X}^T \mathbf{w}_X}\sqrt{\mathbf{w}_Y^T \mathbf{Y}\mathbf{Y}^T \mathbf{w}_Y}} \tag{2}$$

The attended target stimulus was identified by finding the stimulation frequency whose reference signal yielded the maximal canonical correlation with the EEG data.

To further enhance the processing, the FBCCA was used [14], in which a filter bank analysis first performed sub-band decompositions on the EEG data with different pass-bands. Four sub-bands were used, all stopping at $48\,\text{Hz}$. To accommodate for the higher difference between the stimulation frequencies, the bands started at $2\,\text{Hz}$, $6\,\text{Hz}$, $10\,\text{Hz}$, and $14\,\text{Hz}$, respectively. After this filtering, the CCA procedure from above was used on each of the sub-band components. This resulted in canonical correlation coefficients between the sub-band components and the reference signals of all stimulation frequencies. To achieve a final score for each target, a weighted summation was performed. The weighting function was defined as follows $w_i = (i+1)^{-1.25} + 0.25$, where i is the sub-band index. Then, the target with the highest ρ_t is classified as the attended stimulus.

Several window lengths were tested, starting from $0.25\,\text{s}$ after stimulus onset, extended with steps of $0.25\,\text{s}$, to the end of stimulation ($3.0\,\text{s}$). This was done for each of the 6 trials. To get a final average accuracy per participant, the average over trials was taken for each time window.

G. Questionnaire

Participants' subjective feedback was collected with a multi-part questionnaire. Following each experimental condition, participants rated their fatigue, discomfort, eye strain and ease of concentration on a 6-point Likert-scale. After completion of all conditions, a final questionnaire was presented to gather summative and comparative feedback. It assessed overall comfort and focus, identified which condition was perceived as most disturbing and causing the least eye strain and asked for a final preference for stimulus shape and movement. It furthermore included questions on the VR system itself, including comfort, motion sickness and whether the stimuli were perceived as three-dimensional.

III. Results

A. Frequency Responses and Accuracy

To investigate the frequency responses of the participants, the SNR spectra of all participants per condition are plotted in Figures 2 (a), (c), and (e). It can be observed that the stimulation frequency and its harmonics are well presented for most of the participants. For some participants, however, no such response was observed. Specifically, one participant presented obvious and strong frequency peaks for one specific stimulus frequency ($7.5\,\text{Hz}$) for every trial. Four others did not show clear peaks at any stimulation frequency, or similarly, only one frequency response to each trial. The SNR spectra revealed that average peak SNR values were highest for the SSVEP condition compared to the zooming and rotating. Furthermore, the analysis showed distinct relationships between the fundamental frequency and the first harmonic. Specifically, in the SSVEP condition, the fundamental frequency's SNR was consistently greater than that of its first harmonic. Conversely, for the moving stimuli, this relationship depended on the shape. For the cubes, the first harmonic's SNR was dominant during rotating, and mostly during zooming. For the diamonds, however, the fundamental frequency's SNR was dominant in the zooming, but no consistency was found for rotation. For comparing the shapes, in the SSVEP condition, the diamonds yielded higher SNR values than cubes at specific frequencies: for both the fundamental and its first harmonic at the middle frequencies, for the fundamental at the highest frequency, and for the first harmonic at the lowest frequency. In contrast, during both moving conditions, cubes consistently produced a stronger SNR for the first harmonic. For the fundamental frequency neither shape showed consistent dominance over the other.

Figures 2 (b), (d), and (f) present the average accuracy and the accuracy per participant, over time. The participant mentioned above, who had peaks at $7.5\,\text{Hz}$ in each trial, is not included in these accuracy plots. For the longest time window of length $2.75\,\text{s}$ ($3.0 - 0.25\,\text{s} = 2.75\,\text{s}$), the cubes had

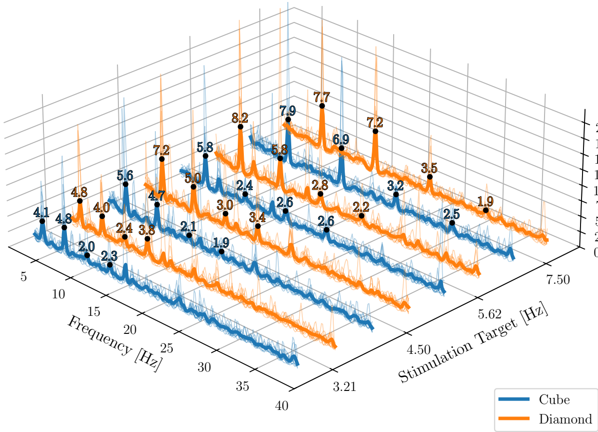

(a) SSVEP- Frequency responses

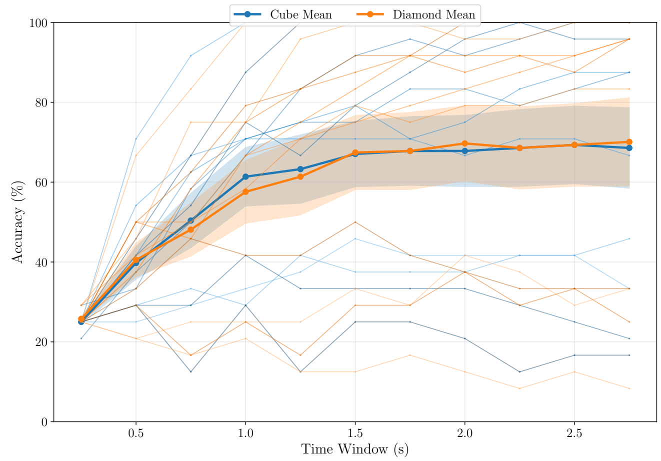

(b) SSVEP - Average accuracy

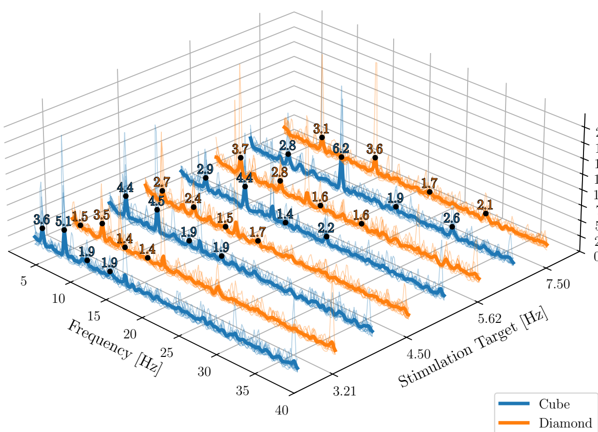

(c) Rotate - Frequency responses

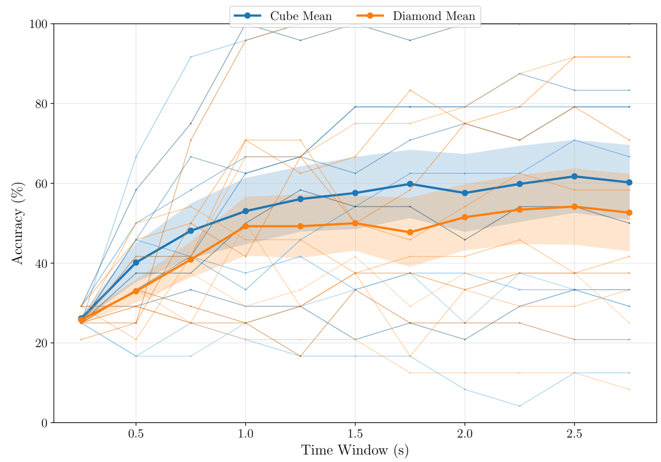

(d) Rotate - Average accuracy

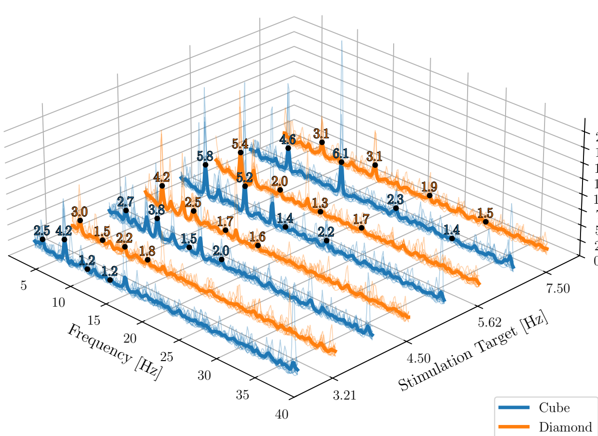

(e) Zoom - Frequency responses

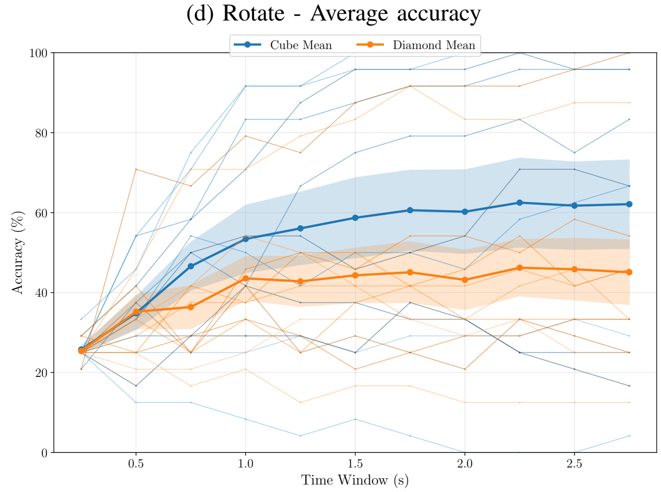

(f) Zoom - Average accuracy

Fig. 2: **Offline analysis for all conditions.** The graphs present the offline results for the 3D shape and stimulation conditions. In all plots, blue represents the cubes, and orange the diamonds. The first three plots (a), (c), (e) show the frequency responses using the calculated SNR spectra. The tick lines show the average response over participants, the thinner lines show the responses of individual participants. The black dots denote the fundamental frequency and its harmonics, together with the average SNR value in text. The last three figures (b), (d), (f) show the mean accuracy over time for 11 out of the 12 participants, calculated using different time windows. Similarly, the thick line presents the mean over participants, together with the standard error band shaded around, and the thin lines represent the individual responses for each participant.

an average accuracy of 62.12% for zoom, 60.23% for rotate, and 68.56% for SSVEP. The diamonds resulted in 45.08% (zoom), 52.65% (rotate), and 70.08% (SSVEP). For the $1.50\,\mathrm{s}$ time window, the cubes reached an average accuracy of 58.71%, 57.58%, and 67.05%, respectively. The diamonds 44.32% (zoom), 50.00% (rotate), and 67.42% (SSVEP). In all conditions, approximately four participants did not reach accuracies higher than 40%. Their corresponding frequency spectra showed low SNR values at the stimulation frequencies or their harmonics. From the plots above, it can furthermore be observed that the diamond shape, shown in orange, mainly reached lower average accuracies than the cubes for the rotate and zoom condition. For SSVEP, the cubes and diamonds, on average, reached similar accuracies.

B. Questionnaire Results

The results of the questionnaire, presented in Figure 3, showed that, on average, the rotating diamond was rated as the most comfortable stimulus and caused the least eye strain. The SSVEP cube was perceived to be the easiest to concentrate on. Then, the zooming cube condition reached the lowest subjective comfort, was perceived to cause the most eye straining, and was the hardest to concentrate on. On average, the participants reported the VR system to be comfortable to wear, and all but one participant, reported to not have perceived any motion sickness. Overall, all subjects perceived the shapes as 3D objects. Lastly, in terms of final preference, seven participants reported to prefer the cubes, five the diamonds. Additionally, eight preferred rotation, three the SSVEP flickering, and one the zooming.

IV. Discussion

This study aimed to investigate the introduction of 3D stimuli and movements for a VR-based SSMVEP BCI system. Two shapes, a cube and a diamond, were modulated with either flickering (SSVEP), or by zooming or rotating (SSMVEP). The experiment was presented in an HMD.

All conditions were able to evoke clear responses at the stimulation frequency and its harmonics. The frequency SNR spectrum showed that the SSVEP condition evoked higher SNR values than both SSMVEP conditions, deviating from the reported finding by Gao and colleagues [15]. In terms of performance, SSVEP reached, on average, higher accuracies than both movements and shapes. However, this performance is lower than usually reported in SSVEP literature. Furthermore, several participants did not achieve high performance under any of the conditions. This fact, and SSVEP's low accuracy, shows the need for testing this during an online experiment, such that the participant can receive live feedback from the system and change their approach. When comparing the SSMVEP conditions, the performances were on average comparable, specifically between the movements themselves. However, for the shapes, the cubes consistently reached a higher overall accuracy for all time windows. This might be due to the difference in the stimuli's geometry. Although the diamonds shared the same maximum width and depth as the cubes, their height was increased to compensate for the smaller perceived volume due to its elongated and tapering shape. This difference in geometry also resulted in a dissimilar application of the checkerboard texture across the stimuli's surfaces. However, it should be noted that in the SSVEP condition both shapes reached similar performances. Additionally, the lowest stimulation frequency ($3.214\,\mathrm{Hz}$) has previously been shown to underperform compared to higher frequencies [16], possibly influencing the performance. On the other hand, the highest stimulation frequency resulted in a less fluid movement, due to the limited number of frames for the movement. However, these stimulation frequencies were chosen to comply with the HMD's refresh rate and the SSMVEP motion requirements.

The questionnaire revealed that the participants preferred the rotating diamond, causing the least eye strain. However, it did not reach high accuracies for all participants. Nonetheless, for some it was able to evoke strong responses with high SNRs and performed well in terms of accuracy. When selecting a stimulus for the SSMVEP protocol, a personalised stimulus selection could be an interesting approach. The zooming stimulus was rated the least comfortable and most difficult to focus on, presumably because the movement's amplitude was quite large. This shows the need for designing other movements, that evoke a strong response without being too intense and thereby decreasing the user comfort.

SSMVEP is proposed as an alternative to SSVEP to alleviate fatigue caused by flickering stimuli [2]. In this study, participants were only exposed to each condition for around three minutes, limiting our ability to draw conclusions about long-term fatigue. However, subjectively, participants reported feeling less tired after observing the rotating diamond. An additional limitation is the small sample size, which further restricted the ability to draw any strong conclusions. A future study involving 3D stimuli for SSMVEP in VR should use a bigger sample size. Lastly, here, the training-free FBCCA method was used, specifically, using the sine and cosine templates as reference signals to calculate the canonical correlation coefficients. However, a method using subject-specific training might be able to extract the responses needed for those participants who reached lower accuracies in this study. Furthermore, here the maximum data length that could be used per trial was restricted by the recorded $3\,\mathrm{s}$ data, where perhaps some participants might have needed more time to sufficiently focus on the target.

This study provided initial insights into using 3D-shaped stimuli within a VR-based BCI employing the SSMVEP paradigm. Future research should implement an online system to create a closed-loop experience that offers real-time user feedback. Additionally, decoding accuracy could be enhanced by adopting methods better suited for SSMVEP response decoding. The stimulus presentation should be integrated into immersive virtual environments to fully leverage VR capabilities. Finally, subsequent work should investigate an expanded repertoire of motion types and shapes, exploring VR's unique potential to present stimuli beyond traditional 3D shapes like cubes, spheres, and diamonds, incorporating more sophisticated and varied object forms.

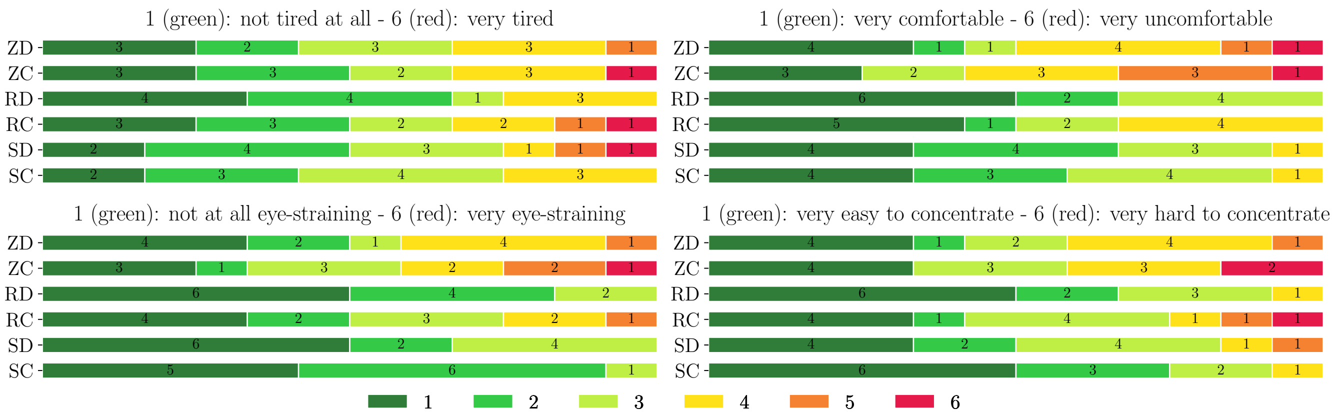

Fig. 3: **Questionnaire answers.** Each plot shows the answers to the corresponding question, which was answered on a 1-6 scale, plotted as dark green (1) to red (6). The abbreviations are as follows: zoom-diamond (ZD), zoom-cube (ZC), rotate-diamond (RD), rotate-cube (RC), SSVEP-diamond (SD), SSVEP-cube (SC).

V. Conclusions

In this study, three-dimensional shapes were implemented in a VR environment and were presented to subjects according to the SSMVEP paradigm. The cube and diamond stimuli were able to evoke clear SNR peaks at the stimulation frequency and its harmonics, but did not result in a high performance for all participants. Specifically, the SSVEP protocol reached higher average accuracies than both SSMVEP conditions. This study shows the potential of using 3D stimuli with SSMVEP stimulation for a VR implementation, the user preference for the SSMVEP paradigm, and that an individualised approach might be beneficial to the user's comfort and system performance.

VI. Acknowledgment

This work was supported by the European Union's research and innovation programme under the Marie Skłodowska-Curie grant agreement No 101118964. The authors thank the financial support provided by "The Friends of the University Rhine-Waal - Campus Cleve" association.

References

[1] Wolpaw, J., Birbaumer, N., McFarland, D., Pfurtscheller, G. & Vaughan, T., "Brain–computer interfaces for communication and control." *Clinical Neurophysiology*, **113**, (6), pp. 767-791, Jun. 2002. 10.1016/S1388-2457(02)00057-3

[2] Xie, J., Xu, G., Wang, J., Zhang, F. & Zhang, Y., "Steady-State Motion Visual Evoked Potentials Produced by Oscillating Newton's Rings: Implications for Brain-Computer Interfaces." *PLoS ONE.*, **7**, (6), p. e39707, Jun. 2012. 10.1371/journal.pone.0039707

[3] Chai, X., Zhang, Z., Guan, K., Liu, G. & Niu, H., "A Radial Zoom Motion-Based Paradigm for Steady State Motion Visual Evoked Potentials." *Frontiers In Human Neuroscience*, **13**, Apr. 2019. 10.3389/fnhum.2019.00127

[4] Koo, B., Lee, H., Nam, Y. & Choi, S., "Immersive BCI with SSVEP in VR head–mounted display." in *2015 37th Annual International Conference Of The IEEE Engineering In Medicine And Biology Society (EMBC)*. IEEE, Aug. 2015. 10.1109/EMBC.2015.7318558

[5] Stawicki, P., Gembler, F., Chan, C., Benda, M., Rezeika, A., Saboor, A., Grichnik, R. & Volosyak, I., "SSVEP-Based BCI in Virtual Reality - Control of a Vacuum Cleaner Robot." in *2018 IEEE International Conference On Systems, Man, And Cybernetics (SMC)*. IEEE, Oct. 2018. 10.1109/smc.2018.00749

[6] Zeng, X., Zhu, G., Yue, L., Zhang, M. & Xie, S., "A Feasibility Study of SSVEP–Based Passive Training on an Ankle Rehabilitation Robot." *Journal Of Healthcare Engineering*, **2017**, pp. 1-9, 2017. 10.1155/2017/6819056

[7] Ravi, A., Lu, J., Pearce, S. & Jiang, N., "Asynchronous SSMVEP BCI and Influence of Dynamic Background in Augmented Reality." in *2021 27th International Conference On Mechatronics And Machine Vision In Practice (M2VIP)*. IEEE, pp. 340-343, Nov. 2021. 10.1109/M2VIP49856.2021.9665078

[8] Ravi, A., Lu, J., Pearce, S. & Jiang, N., "Enhanced System Robustness of Asynchronous BCI in Augmented Reality Using Steady-State Motion Visual Evoked Potential." *IEEE Transactions On Neural Systems And Rehabilitation Engineering*, **30**, pp. 85-95, 2022. 10.1109/TNSRE.2022.3140772

[9] Liu, J., Xie, J., Zhang, H., Yang, H., Shao, Y. & Chen, Y., "Improvement of BCI performance with bimodal SSMVEPs: enhancing response intensity and reducing fatigue." *Frontiers In Neuroscience*, **19**, Mar. 2025. 10.3389/fnins.2025.1506104

[10] Zhang, X., Xu, G., Xie, J., Li, M., Pei, W. & Zhang, J., "An EEG–driven Lower Limb Rehabilitation Training System for Active and Passive Co–stimulation." in *2015 37th Annual International Conference Of The IEEE Engineering In Medicine And Biology Society (EMBC)*. IEEE, pp. 4582-4585, Aug. 2015. 10.1109/EMBC.2015.7319414

[11] "Unity Technologies: Unity Game Engine version 6000.0.31f1." URL: https://unity3d.com Accessed on 29.04.2025

[12] McFarland, D., McCane, L., David, S. & Wolpaw, J., "Spatial filter selection for EEG-based communication." *Electroencephalography And Clinical Neurophysiology*, **103**, (3), pp. 386-394, Sept. 1997. 10.1016/s0013-4694(97)00022-2

[13] Xie, J., Xu, G., Luo, A., Li, M., Zhang, S., Han, C. & Yan, W., "The Role of Visual Noise in Influencing Mental Load and Fatigue in a Steady-State Motion Visual Evoked Potential-Based Brain-Computer Interface." *Sensors*, **17**, (8), p. 1873, Aug. 2017. 10.3390/s17081873

[14] Chen, X., Wang, Y., Gao, S., Jung, T. & Gao, X., "Filter bank canonical correlation analysis for implementing a high-speed SSVEP-based brain computer interface." *Journal Of Neural Engineering*, **12**, (4), p. 046008, Jun. 2015. 10.1088/1741-2560/12/4/046008

[15] Gao, Y., Ravi, A. & Jiang, N., "Effect of Competing Stimuli for Steady-State Visually Evoked Potential and Steady-State Motion Visually Evoked Potential." *IEEE Access*, **9**, pp. 129820-129829, 2021. 10.1109/ACCESS.2021.3112218

[16] Stawicki, P., Rezeika, A., Saboor, A. & Volosyak, I., "Investigating Flicker-Free Steady-State Motion Stimuli for VEP-Based BCIs." in *2019 E-Health And Bioengineering Conference (EHB)*. IEEE, Nov. 2019. 10.1109/ehb47216.2019.8969970